Oscillator strength of trion states in ZnSe-based quantum wells

G. V. Astakhov,[1] V. P. Kochereshko,[1] D. R. Yakovlev,[1,2] W. Ossau,[2] J. Nürnberger,[2] W. Faschinger,[2] and G. Landwehr[2]
[1]*A. F. Ioffe Physical-Technical Institute RAS, 194021, St. Petersburg, Russia*
[2]*Physikalisches Institut der Universität Würzburg, 97074, Würzburg, Germany*
(Received 18 February 2000)

The oscillator strength of negatively charged excitons (trions) in ZnSe/(Zn,Mg)(S,Se) quantum-well structures with *n*-type modulation doping is studied by means of reflectivity as a function of electron concentration, temperature, and external magnetic fields. The trion oscillator strength is found to increase linearly with increasing electron concentration up to $6\times10^{10}\,\mathrm{cm}^{-2}$. The trion nonradiative damping shows no dependence on the electron concentration or external magnetic field. An optical method, based on the analysis of the polarization of the trion line, is proposed to investigate two-dimensional electron gases of low density from 10^9 up to $10^{11}\,\mathrm{cm}^{-2}$.

A negatively charged exciton complex (trion) in semiconductors, consisting of an exciton attracting an additional electron, was predicted theoretically in 1958.[1] This state has been under intensive study since 1993, when the first experimental proof of the existence of trions in quantum-well (QW) structures was reported.[2] Trions have been observed in QW structures based on different semiconductor compounds, such as CdTe,[2,3] GaAs,[4] and ZnSe.[5,6] Negatively and positively charged trions related both to heavy-hole and light-hole excitons have been studied experimentally.[3,6,7] Coherent and recombination dynamics of the trion states are actual topics of ongoing research in this field.[8,9] Theoretical works supporting the experimental studies are also in progress.[10] However, quite a number of features of the trion states are not understood yet and/or are the subject of controversy.

In particular, an important problem of the trion and exciton oscillator strengths at various concentrations of free carriers in QW's has been raised in a number of publications (see Refs. 3, 10, 11, and 12). However, detailed experimental investigations of this problem have been published only very recently. They are exemplified by the positively charged excitons (X^+) in CdTe-based QW's embedded in a microcavity[13] and in semimagnetic (Cd,Mn)Te QW's.[14,15] In both papers an oscillator strength ''transfer'' (i.e., redistribution of oscillator strength) between exciton and X^+ resonances dependent on the concentration of free holes was established experimentally. In these studies the experimentally measured Moss-Burstein shift was used to evaluate the density of the hole gas. This method is limited to the range of high concentrations (above $6\times10^{10}\,\mathrm{cm}^{-2}$) and for lower concentrations hole densities were estimated via model calculations.[15]

In this paper we present detailed experimental investigations on the modification of the negatively charged exciton (X^-) and neutral exciton (X) resonances in the presence of a low-density two-dimensional electron gas (2DEG) with concentration n_e varying from 5×10^9 up to $1.2\times10^{11}\,\mathrm{cm}^{-2}$. An optical method to characterize the low-density 2DEG, based on the analysis of trion polarization in external magnetic fields, was developed. The oscillator strength of the exciton and trion is treated from the point of view of their resonant contribution to the dielectric function of the crystal. Reflectivity spectroscopy is used as the most reliable and informative technique. The radiative and nonradiative damping of trions and excitons was examined as a function of electron concentration, external magnetic field, and temperature. We chose modulation-doped ZnSe/(Zn,Mg)(S,Se) quantum-well structures as a model system for this study. The choice of ZnSe-based QW's with strong Coulomb interaction, as compared with GaAs- or CdTe-based QW's, allows us to observe very pronounced exciton and trion resonances in the reflectivity spectra and to provide high experimental accuracy for calculated parameters.

I. EXPERIMENT

$ZnSe/Zn_{0.89}Mg_{0.11}S_{0.18}Se_{0.82}$ single QW (SQW) structures were grown by molecular-beam epitaxy on (100)-oriented GaAs substrates (for details of growth and optical properties, see Ref. 6). An 80-Å-thick ZnSe SQW was embedded between 1000- and 500-Å-thick $Zn_{0.89}Mg_{0.11}S_{0.18}Se_{0.82}$ barriers. The total band-gap discontinuity of 200 meV between the QW and the barrier materials was distributed approximately evenly between the conduction- and valence-band edges. One structure was nominally undoped with a residual electron concentration of $n_e\leqslant10^{10}\,\mathrm{cm}^{-2}$ in the SQW, due to the weak *n*-type background conductivity of the barriers. A set of modulation-doped structures with a 2DEG concentration in the range from $n_e=3\times10^{10}\,\mathrm{cm}^{-2}$ up to $1.2\times10^{11}\,\mathrm{cm}^{-2}$ were grown with a Cl-doped layer separated from the QW by a 100-Å-thick spacer. Most of the reflectivity measurements were performed at normal incidence and only some spectra were taken under Brewster angle incidence in order to analyze transitions with very weak oscillator strength.[16] Reflectivity spectra were taken at 1.6 K in magnetic fields up to $B=7.5\,\mathrm{T}$ applied in Faraday geometry and at $B=0\,\mathrm{T}$ in a temperature range from 1.6 up to 35 K. Circularly polarized light was analyzed by means of achromatic quarter-wave plates. The signal was dispersed by a 1-m spectrometer and detected by a charged-coupled device (CCD camera).

II. EXPERIMENTAL RESULTS

A. Reflectivity spectra of trions and excitons

Reflectivity spectra of modulation-doped QW's with different 2D electron concentrations are shown in Fig. 1 for

0163-1829/2000/62(15)/10345(8)/$15.00 PRB 62

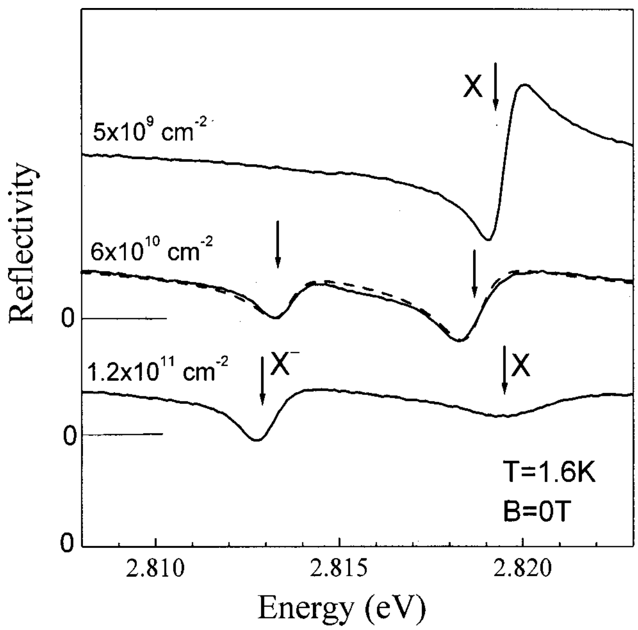

FIG. 1. Reflectivity spectra taken from 80-Å $ZnSe/Zn_{0.89}Mg_{0.11}S_{0.18}Se_{0.82}$ SQW's with different electron concentrations in zero magnetic field. Arrows indicate the resonance energies of excitons (X) and trions (X^-). The best fit with parameters $\Gamma_0^X = 170\ \mu$eV, $\Gamma^X = 0.73$ meV, $\Gamma_0^T = 68\ \mu$eV, and $\Gamma^T = 0.6$ meV is shown by a dashed line. $T = 1.6$ K.

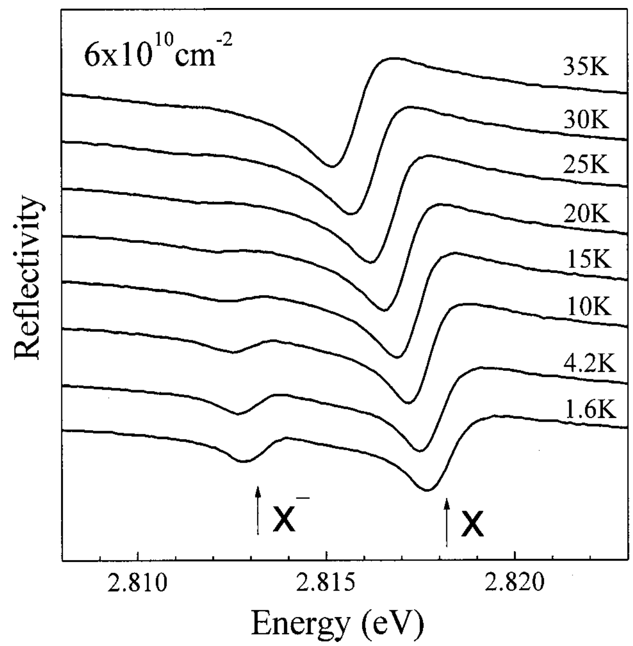

FIG. 2. Reflectivity spectra taken from an 80-Å $ZnSe/Zn_{0.89}Mg_{0.11}S_{0.18}Se_{0.82}$ SQW with $n_e = 6\times10^{10}\ \mathrm{cm}^{-2}$ at different temperatures. $B = 0$ T.

zero magnetic field. Details of the identification of trion transitions and basic trion properties in ZnSe-based QW's were published in Refs. 5 and 6. In the nominally undoped sample (upper spectrum) only a single strong resonance, which corresponds to a heavy-hole exciton (X) in the QW, is detectable at normal incidence of the reflected light. In doped samples (middle and lower spectra), a new resonance of a negatively charged exciton (X^-) appears at about 5 meV on the low-energy side from the exciton line. The amplitude of the trion resonance grows with increasing electron concentration. In turn, this is accompanied by a reduction of exciton-resonance amplitude. At high electron concentrations (above $2\times10^{11}\ \mathrm{cm}^{-2}$) the exciton line disappears from the reflectivity spectra.

Parameters of the exciton and trion resonances [i.e., resonance frequency (ω_0), radiative damping (Γ_0), and nonradiative damping (Γ)], which govern their contribution to the dielectric function, were deduced from a best fit of experimental reflectivity spectra to the calculated ones in the framework of the non-local dielectric response theory.[17,18] This approach was successfully used for the reflectivity analysis of undoped QW's.[16,17] An example of such a fit is shown by the dotted line in Fig. 1. Γ_0 and Γ determined by this procedure for different temperatures, magnetic fields, and electron concentrations are presented in Figs. 3, 5, 8, and 9.

Following Ivchenko and co-workers[18,19] the exciton-resonant reflection coefficient in a SQW is given by

$$r = \frac{i\Gamma_0}{\omega_0 - \omega - i(\Gamma + \Gamma_0)}. \tag{1}$$

In this case the radiative damping Γ_0 has a physical meaning, namely, the exciton oscillator strength in the QW. It is proportional to the exciton oscillator strength per unit volume (F_X) used in Refs. 20 and 21, i.e., $\Gamma_0 \propto F_X$. It is worth noting here the relation between the exciton radiative damping and the exciton radiative lifetime (τ_{rad}), $\Gamma_0^X = \frac{1}{2}\ \tau_{\mathrm{rad}}$.[18]

The nonradiative damping constant Γ is characteristic for the broadening of the exciton resonance. It includes all broadening mechanisms with the exception of the radiative broadening, which is controlled by Γ_0. At low temperatures, when the exciton-phonon scattering is negligible, and in undoped QW's Γ is dominated by inhomogeneous broadening, which, in turn, mainly arises from well-width fluctuations and alloy fluctuations in barriers. In QW's with a 2DEG exciton-electron scattering could cause considerable homogeneous broadening of exciton states.[22] This mechanism is spin dependent and, as we will show, is important for the studied ZnSe-based QW's.

A set of reflectivity spectra measured in a SQW with $n_e = 6\times10^{10}\ \mathrm{cm}^{-2}$ is shown in Fig. 2 for different temperatures in the range from 1.6 up to 35 K. With increasing temperature the trion resonance becomes weaker and becomes unresolvable at $T \geqslant 25$ K. In contrast the exciton resonance increases its amplitude. A weak energy shift of the resonances is due to the temperature-induced narrowing of the energy gap.

Temperature dependencies of the radiative and nonradiative damping for excitons and trions are plotted in Fig. 3. One can see that the vanishing of the X^- resonance is caused by two factors: a decrease of Γ_0 and an increase of Γ. It is interesting to note that the decrease of the trion damping constant Γ_0^T (from 68 μeV at 1.6 K down to 0 μeV at 30 K) is accompanied by an increase of the exciton damping Γ_0^X (from 170 μeV at 1.6 K up to 210 μeV at 30 K) in a way that a sum $\Gamma_0^X + \Gamma_0^T$ is about constant. Finally, the nonradiative damping of excitons $\Gamma^X = 0.7$ meV was found to be temperature independent.

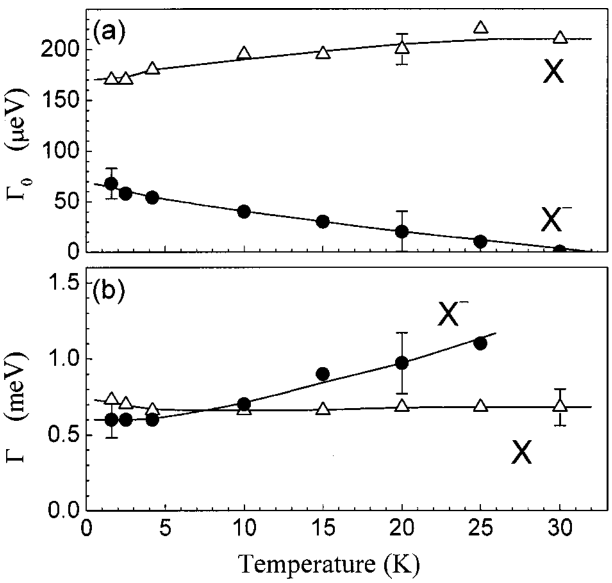

FIG. 3. Radiative (Γ_0) and nonradiative (Γ) damping of exciton and trion states in an 80-Å ZnSe/$Zn_{0.89}Mg_{0.11}S_{0.18}Se_{0.82}$ SQW with $n_e = 6\times10^{10}\,\mathrm{cm}^{-2}$ as a function of temperature.

The modification of reflectivity spectra in magnetic fields is shown in Fig. 4 for two circular polarizations σ^- and σ^+, corresponding to different spin orientations of excitons and trions. In the undoped structure no changes of the exciton oscillator strength (i.e., Γ_0^X) was detected. The exciton line shows a weak diamagnetic shift of 0.25 meV at $B=7$ T (Ref. 5) and is split in two Zeeman components with an exciton g factor $g_{\mathrm{exc}}=+0.38$.[6] However, in the doped structures both the trion and exciton resonances became strongly polarized.

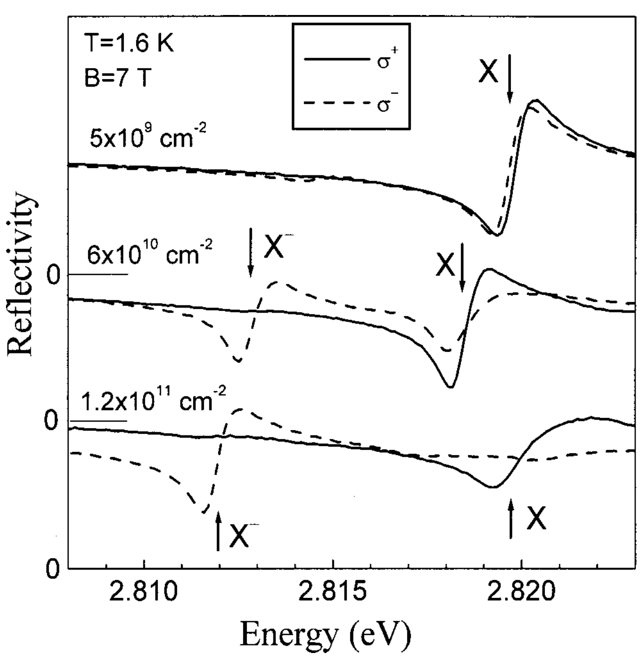

FIG. 4. Reflectivity spectra taken from 80-Å ZnSe/$Zn_{0.89}Mg_{0.11}S_{0.18}Se_{0.82}$ SQW's with different electron concentrations detected in σ^+ (solid) and σ^- (dotted) circular polarizations at a magnetic field of 7 T. $T=1.6$ K.

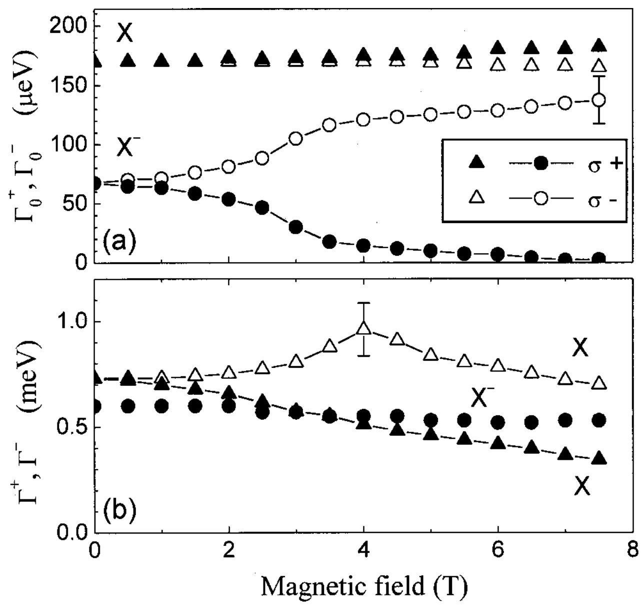

FIG. 5. Magnetic-field dependence of radiative (Γ_0) and nonradiative (Γ) damping for the exciton (triangles) and trion (circles) states in an 80-Å ZnSe/$Zn_{0.89}Mg_{0.11}S_{0.18}Se_{0.82}$ SQW with $n_e = 6\times10^{10}\,\mathrm{cm}^{-2}$. σ^+ and σ^- circular polarized components are shown by solid and open symbols, respectively.

The polarization of the trion line reflects specifics of its spin structure.[2] Being composed of two electrons and one hole, the trion ground state has a singlet configuration with two electron spins oriented antiparallel to each other. The triplet state with parallel spins is unbound at low magnetic fields. In external magnetic fields applied along the QW growth axis a 2DEG shows spin polarization that, in turn, induces circular polarization of the trion resonances in the reflectivity spectra.[6] The strong circular polarization of the X^- resonance can clearly be seen in Fig. 4. The trion resonance becomes two times stronger in σ^- polarization as compared to its zero-field value (see Fig. 1) and loses its intensity in σ^+ polarization.

In more detail the magnetic-field dependencies of the exciton and trion parameters are shown in Fig. 5 for the SQW with $n_e = 6\times10^{10}\,\mathrm{cm}^{-2}$. The nonradiative damping of trions was found to be independent of the magnetic field and is equal for both spin orientations [see Fig. 5(b)]. By contrast, the exciton nonradiative damping shows a strong dependence both on magnetic field and on polarization. Γ^{X+} (shown by solid triangles) decreases from 0.73 meV at $B=0$ T to 0.35 meV at $B=7.5$ T. Γ^{X-} (open triangles) has a nonmonotonic behavior with a maximum value of about 1 meV at $B=4$ T and a subsequent decrease to 0.7 meV at $B=7.5$ T. A difference between Γ^{X+} and Γ^{X-}, caused by spin-dependent exciton-electron scattering,[22] grows up to $B=4$ T and then saturates at a value of 0.35 meV. It is represented in Fig. 10 by solid circles and will be discussed in more detail in Sec. III.

Exciton radiative damping is weakly varied by applied magnetic fields [see Fig. 5(a)]. Only in fields above 4 T is a small difference shown in oppositely polarized spectra: at $B=7.5$ T $\Gamma_0^{X+}=182\,\mu$eV and $\Gamma_0^{X-}=165\,\mu$eV. For the trion resonance Γ_0^{T+} and Γ_0^{T-}, being detected in different polarizations, symmetrical variations are seen in reference to the

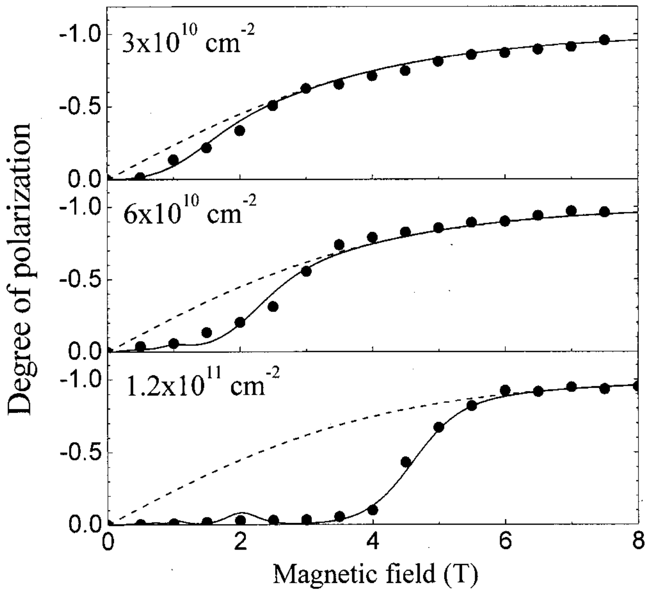

FIG. 6. Magnetic-field-induced circular polarization degree P_c of the trion resonance in reflectivity evaluated for 80-Å $ZnSe/Zn_{0.89}Mg_{0.11}S_{0.18}Se_{0.82}$ SQW's. Dashed lines show the Boltzmann distribution and solid lines trace Fermi-Dirac statistics, which gives the best fits and allows us to determine the electron concentration.

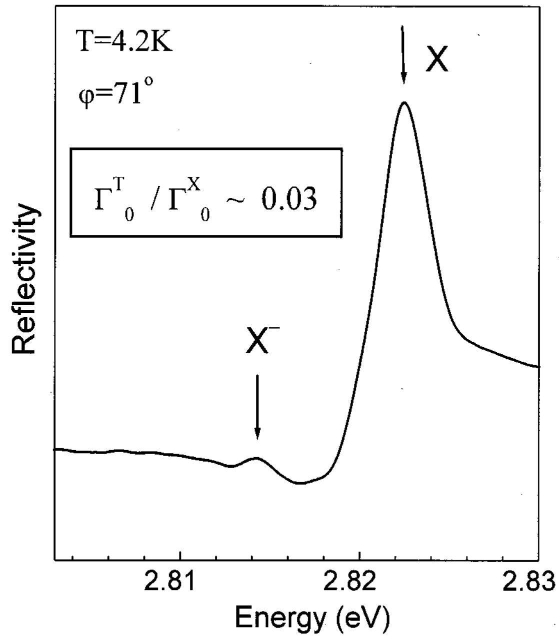

FIG. 7. Reflectivity spectra taken from an undoped SQW at a light incidence close to the Brewster angle. Electron concentration of $n_e = 5\times10^9$ cm^{-2} was evaluated for this structure from the value of the trion radiative damping $\Gamma_0^T = 6$ μeV (see text). $T = 4.2$ K.

zero-field value of $\Gamma_0^T = 68$ μeV, keeping the sum value of $\Gamma_0^{T+} + \Gamma_0^{T-}$ constant for all magnetic fields used.

The enhancement of Γ_0^{T-} (suppression of Γ_0^{T+}) with increasing magnetic field reflects the increase (decrease) of electron concentration for the corresponding spin component. Therefore, the degree of circular polarization of the trion resonance calculated as $P_c = (\Gamma_0^{T+} - \Gamma_0^{T-})/(\Gamma_0^{T+} + \Gamma_0^{T-})$ corresponds to a polarization of a 2DEG in external magnetic fields. Experimentally measured $P_c(B)$ dependencies are plotted by circles in Fig. 6 for QW's with different electron concentrations. These results allow us to get information not only about the polarization of a 2DEG but also about the 2DEG density.

B. Optical method to determine the 2DEG concentration

In this part we describe optical methods to determine 2DEG densities in QW's for n_e in the range from 10^9 up to about 2×10^{11} cm^{-2}. The experimental results shown by dots in Fig. 6 represent the polarization degree of a 2DEG in QW's. At very low electron concentrations ($n_e < 10^{10}$ cm^{-2}), when the Fermi energy $\varepsilon_F < k_B T$, the electron polarization is well described by a Boltzmann distribution of electrons on the Zeeman sublevels. The Boltzmann distribution calculated for $T = 1.6$ K with an electron g factor $g_e = +1.14$ (Ref. 6) is shown in Fig. 6 by dotted lines. A clear deviation of the experimental data from the Boltzmann distribution is seen at low magnetic fields, increasing for higher electron concentrations. For the highest concentration studied here ($n_e = 1.2\times10^{11}$ cm^{-2}) the trion resonance is completely unpolarized in magnetic fields below 4 T. Fermi-Dirac statistics, accounting properly for the properties of a degenerate electron gas, was used for the calculation of the polarization. A good agreement with experimental data was achieved (see solid lines in Fig. 6). The Fermi energy was the only fitting parameter in this calculation. In turn, the Fermi energy is directly linked with the electron concentration via $\varepsilon_F = \pi\hbar^2 n_e / m_e$. In ZnSe-based QW's the effective mass of conduction-band electrons is $m_e = 0.16 m_0$ and $\varepsilon_F = 1.44\times10^{-12} n_e$, where ε_F is given in meV and n_e in cm^{-2}. Therefore, fitting the experimental points from Fig. 6 with the polarization based on the Fermi-Dirac statistics allowed us to determine the 2DEG density. In the modeling we assume that the Fermi level is pinned by the donors in the modulation-doped layer. (This is valid for our ZnSe-based QW's with relatively small band offsets. Detailed discussion on the validity of this assumption will be presented elsewhere.) For the ZnSe-based QW's under study this method allows us to determine the electron density in QW's with n_e down to 2×10^{10} cm^{-2}.

At lower electron densities the difference between the Fermi-Dirac and the Boltzmann distribution is too small to allow an accurate determination of n_e. In this case the electron density can be determined by means of the linear dependence of the trion radiative damping on n_e with $\Gamma_0^T/n_e = 1.16\times10^{-9}$ μeV cm^2 measured for ZnSe-based QW's in this paper (see Sec. II C). Our goal is to measure Γ_0^T with high accuracy. Modulation spectroscopy and/or reflectivity measurements under Brewster angle[16,18] extend significantly the sensitivity of the light-reflection technique and allow us to detect transitions with low oscillator strength.

As an example a reflectivity spectrum of an undoped SQW taken under incident angle $\varphi = 71°$, which is close to the Brewster angle of $\varphi_{\mathrm{Br}} = 69°$, is shown in Fig. 7. The radiative damping of the trion $\Gamma_0^T = 6$ μeV is only 3% of the exciton radiative damping. The electron concentration in this structure found accounting to the relation n_e

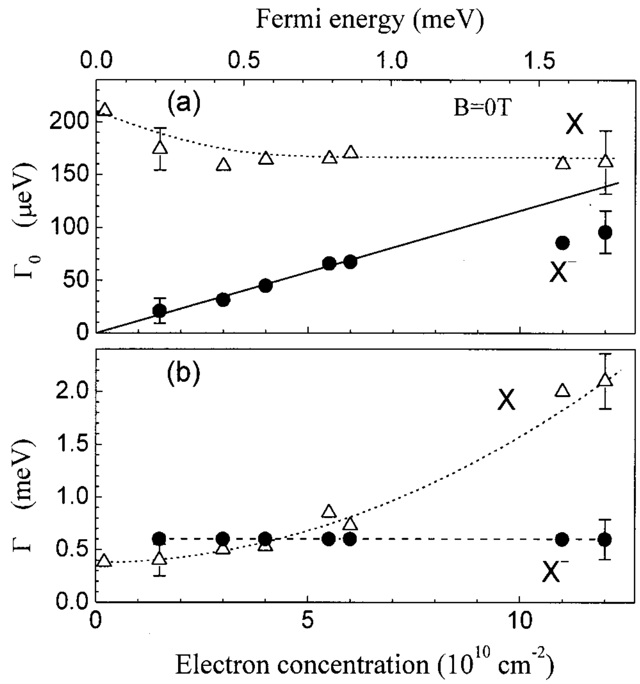

FIG. 8. Radiative (Γ_0) and nonradiative (Γ) damping of the exciton and trion states in 80-Å $ZnSe/Zn_{0.89}Mg_{0.11}S_{0.18}Se_{0.82}$ SQW's as a function of the electron concentration at zero magnetic fields. Dashed and dotted lines are given as guide to the eye. The solid line is a linear interpolation of experimental data for trions for $n_e \leqslant 6\times10^{10}\,\mathrm{cm}^{-2}$. $T=1.6$ K.

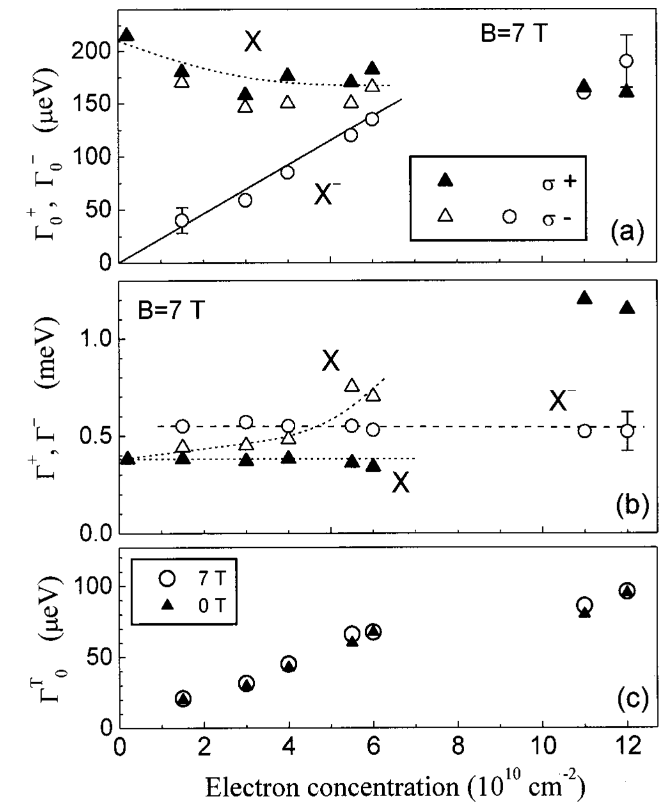

FIG. 9. (a) Radiative (Γ_0) and (b) nonradiative (Γ) damping of the exciton and trion states in 80-Å $ZnSe/Zn_{0.89}Mg_{0.11}S_{0.18}Se_{0.82}$ SQW's as a function of the electron concentration at a magnetic field of 7 T. The solid line in the (a) panel has a slope of $2.32\times10^{-9}\,\mu\mathrm{eV\,cm}^2$. (c) Comparison of the trion radiative damping measured at $B=0$ and 7 T and treated with Eq. (2). $T=1.6$ K.

$=\Gamma_0^T/(1.16\times10^{-9})$ is equal to $5\times10^9\,\mathrm{cm}^{-2}$. We believe that n_e values as low as $10^9\,\mathrm{cm}^{-2}$ can be measured by means of the suggested procedure.

C. Exciton and trion parameters as a function of 2DEG concentration

Now, having an optical method of measuring n_e, we analyze parameters of the exciton and trion resonances as functions of the 2DEG density. $\Gamma_0(n_e)$ and $\Gamma(n_e)$ dependencies measured at zero magnetic field are plotted in Fig. 8. It is remarkable that the trion radiative damping Γ_0^T (i.e., the trion oscillator strength) increases linearly with electron concentrations up to $n_e\approx6\times10^{10}\,\mathrm{cm}^{-2}$ [see closed circles in Fig. 8(a)]. This result is intuitively expected, as a necessary condition for trion formation is the presence of background electrons in the QW. For this three-particle excitonic complex, one electron and one hole are photogenerated by an absorbed photon and second electron is taken from a 2DEG. For a diluted 2DEG, where the average distance between electrons is larger than the size of the trion orbit, one can expect a linear dependence of the trion generation probability on the electron density.

The solid line in Fig. 8(a) which is a linear interpolation of data points for $n_e\leqslant6\times10^{10}\,\mathrm{cm}^{-2}$, has a slope $\Gamma_0^T/n_e=1.16\times10^{-9}\,\mu\mathrm{eV\,cm}^2$. Data points for $n_e>10^{11}\,\mathrm{cm}^{-2}$ deviate significantly from the linear dependence and show a saturation tendency for $\Gamma_0^T(n_e)$ function.

The exciton radiative damping Γ_0^X decreases from 210 μeV for the undoped QW down to about 170 μeV for $n_e=3\times10^{10}\,\mathrm{cm}^{-2}$ and then remains constant at this level up to $n_e=1.2\times10^{11}\,\mathrm{cm}^{-2}$. Qualitatively the results presented in Fig. 8(a) are in agreement with the idea on oscillator strength ''transfer'' between excitons and trions.[13,15]

The nonradiative broadening of excitons demonstrates a strong dependence on n_e increasing from 0.4 meV in the undoped QW to 2.1 meV for $n_e=1.2\times10^{11}\,\mathrm{cm}^{-2}$. This additional broadening is caused by exciton-electron scattering.[22] Surprisingly, the nonradiative broadening of the trion resonances is rather independent of the electron density [see solid circles in Fig. 8(b)].

Figure 9 is analogous to Fig. 8, but the exciton and trion parameters are given for a magnetic field of $B=7$ T and for two circular polarizations. The exciton radiative damping has a dependence, which is very similar to the zero-field case [compare Figs. 9(a) and 8(a)]. For the trion radiative damping in strong (σ^-) polarization (Γ_0^{T-}) we obtain a linear dependence on n_e with a slope, which is twice larger than that at zero field [the straight solid line in Fig. 9(a) is drawn with a slope of $2.32\times10^{-9}\,\mu\mathrm{eV\,cm}^2$]. However, one should keep in mind that trions are totally polarized at $B=7$ T and $\Gamma_0^{T+}=0$. Taking into account the zero-field value

$$\Gamma_0^T=\frac{\Gamma_0^{T+}+\Gamma_0^{T-}}{2}, \tag{2}$$

we establish that the trion oscillator strengths at $B=0$ and 7 T coincide with each other for the whole range of n_e studied. These results are depicted in Fig. 9(c).

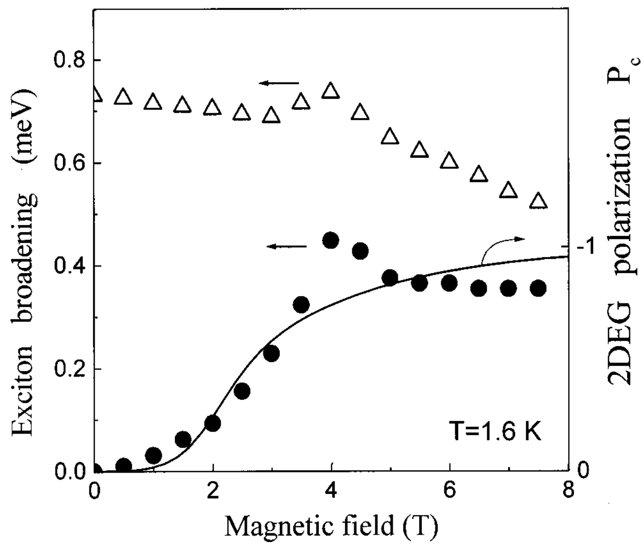

FIG. 10. Spin-independent part of the exciton nonradiative damping $(\Gamma^{X+}+\Gamma^{X-})/2$ (open triangles) and spin-dependent part $\Gamma^{X+}-\Gamma^{X-}$ (solid circles) as a function of magnetic fields. The solid line is taken from the middle panel of Fig. 6. It shows polarization of a 2DEG with $n_e=6\times10^{10}\,\mathrm{cm}^{-2}$.

Similar to the zero-field results from Fig. 8(b) Γ^T is independent of n_e at $B=7$ T [see circles in Fig. 9(b)]. As we have already shown in Fig. 5 the exciton broadening depends strongly on polarization and on the magnetic field value. At $B=7$ T σ^+ polarized excitons have a stable level of $\Gamma^{X+}=0.4$ meV [see solid triangles in Fig. 9(b)], except for data points at $n_e\geq1.1\times10^{11}\,\mathrm{cm}^{-2}$. On the other hand, Γ^{X-} increases rapidly with n_e similar to the $\Gamma^X(n_e)$ dependence at $B=0$ T.

III. DISCUSSION

In this part we concentrate on the discussion of the following aspects:

(i) Electron-density dependence of the trion oscillator strength, i.e., $\Gamma_0^T(n_e)$.

(ii) Transfer of oscillator strength between excitons and trions.

(iii) Broadening of exciton resonances due to exciton-electron interaction.

The radiative damping Γ_0 extracted by us from reflectivity spectra has a physical meaning of an oscillator strength and is proportional to the exciton oscillator strength per unit volume (F_X) used in Refs. 20 and 21, i.e., $\Gamma_0\propto F_X$. Following the approach developed in Refs. 20 and 21 for the oscillator strength of a bound exciton, one can derive the following relationship between the exciton radiative damping (Γ_0^X) and the trion radiative damping (Γ_0^T):

$$\Gamma_0^T=\Gamma_0^X N_e\frac{A_T}{A}=\Gamma_0^X n_e \pi a_T^2. \tag{3}$$

Here N_e is the number of electrons in the QW, A is the area of the QW layer, and $A_T=\pi a_T^2$ is the area of the trion with radius a_T. $n_e=N_e/A$ is the electron concentration. In deriving Eq. (3) we used the fact that the exciton and trion oscillator strength per unit volume equal each other. This is valid for the case when the binding energy of the second electron in the trion is much smaller than the exciton binding energy. For the studied ZnSe-based QW's the difference is about 6 times.

Putting in Eq. (3) the experimentally determined parameters $\Gamma_0^X(n_e\approx0)=210\,\mu$eV and $\Gamma_0^T/n_e=1.16\times10^{-9}\,\mu\mathrm{eV\,cm}^2$ we evaluate the radius of the trion $a_T=132$ Å. For comparison, the in-plane radius of 1s exciton states in the studied QW's is about 40 Å.

At electron concentrations exceeding $n_e^*=1.8\times10^{11}\,\mathrm{cm}^{-2}$ estimated from the condition $\pi n_e^* a_T^2=1$, efficient supression of trions by the 2DEG is expected. We believe that the data points for Γ_0^T at $n_e>10^{11}\,\mathrm{cm}^{-2}$ deviating from the linear dependence plot [see Fig. 8(a)] indicate the approaching of this regime.

We found that the radiative damping of the trion increases linearly with electron concentrations up to $n_e\approx6\times10^{10}\ \mathrm{cm}^{-2}$ [see Figs. 8(a) and 9(a)]. Experimental data in external magnetic fields presented in Fig. 5(a) allow us to conclude that in ZnSe QW's at $n_e\leq6\times10^{10}\,\mathrm{cm}^{-2}$ the phase-space filling (which increases by a factor of 2 for the σ^- polarization when a 2DEG is polarized) has no strong influence on the trion oscillator strength per electron. These experimental findings are in agreement with the experimental results of Ref. 11, where the linear dependence of the X^- integral absorption with electron concentration has been established for CdTe QW's in a magnetic field of 8 T and for a 2DEG filling factors $\nu<1$. A linear dependence of $\Gamma_0^T(n_e)$ has been also reported for X^+ states in (Cd, Mn)Te QW's for hole densities $n_h\leq3.7\times10^{10}\,\mathrm{cm}^{-2}$.[15] However, we cannot confirm the dependence of the trion oscillator strength variation on the 2DEG filling factor reported for CdTe QW's.[11] In our findings the trion oscillator strength depends only on the electron concentration and the observed effect of the magnetic field comes from polarization of the trion line.

An effect of an oscillator strength transfer between exciton and trion states is verified in ZnSe QW's by the temperature [Fig. 3(a)] and electron density [Fig. 8(a)] dependencies of the radiative damping for the excitons and trions. The value of the transfer for the studied range of $n_e\leq1.2\times10^{11}\,\mathrm{cm}^{-2}$ does not exceed 25% of exciton radiative damping at $n_e\approx0$. We suppose that the oscillator strength transfer is caused by an interaction between exciton and trion states via the 2DEG. A trion can lose an electron and transform into an exciton and, in turn, an exciton can capture an electron and transform into trion. Obviously, the strength of the interaction between exciton and trion states is scaled with the 2DEG density. A theoretical treatment of this problem will be presented elsewhere.[23]

We have not observed a decrease of the sum of exciton and trion oscillator strengths (i.e., $\Gamma_0^X+\Gamma_0^T$ value) with increasing n_e. Such a decrease has been reported for CdTe QW's with a 2DEG (Ref. 24) and (Cd, Mn)Te QW's with a 2D hole gas.[15] It has been explained by a reduction of the exciton oscillator strength due to screening and phase-space filling effects. The stronger Coulombic interaction in ZnSe compared with CdTe makes excitons in ZnSe QW's more robust against these destruction factors. It follows from our experimental data that in ZnSe QW's the critical electron concentration to destroy excitons exceeds $1.2\times10^{11}\,\mathrm{cm}^{-2}$, which is the maximal concentration for the structures studied in this paper.

Let us now turn to nonradiative damping of excitons and trions. The trion nonradiative damping shows no dependence on n_e [Fig. 8(b)]. We note that a similar behavior has been reported for X^- in CdTe QW's,[11] and therefore it is not unique for ZnSe QW's. However, this result is very surprising. Trions are charged particles and one can expect their effective interaction with a 2DEG. The reason why this interaction is absent or does not contribute to the broadening of the trion line is not clear and requires further investigation.

The exciton nonradiative damping shown in Fig. 8(b) increases drastically (about 4 times) with n_e. We assign this exciton line broadening to the exciton interaction with 2DEG electrons. In exciton-electron scattering events electrons are excited above the Fermi level and a homogeneous contribution of this mechanism to the exciton linewidth is of the order of ε_F. Indeed, an increase of Γ^X is very close to ε_F values shown in the upper scale of Fig. 8. It is worthwhile to note here that exciton line broadening at high electron densities contributes significantly to the reduction of the amplitude of the exciton reflectivity line (see Fig. 1, $n_e = 1.2\times10^{11}\,\mathrm{cm}^{-2}$).

A pronounced effect of spin-dependent exciton broadening, visualized by a difference between Γ^{X-} and Γ^{X+} in Fig. 5(b) becomes obvious upon polarization of a 2DEG by magnetic fields. In Fig. 10 spin-dependent $\Gamma^{X-}-\Gamma^{X+}$ and spin-independent $(\Gamma^{X-}+\Gamma^{X+})/2$ contributions of the exciton broadening in a SQW with $n_e=6\times10^{10}\ \mathrm{cm}^{-2}$ are plotted. The magnetic-field behavior of the spin-dependent part coincides with the polarization dependence of the 2DEG shown by a solid line in Fig. 10. It increases, reaches the value of about 0.4 meV in magnetic fields of 5 T, and then saturates. The exciton line is broader for σ^- polarization, when an electron spin in the exciton is oriented opposite to the 2DEG polarization. In this case the electron exchange is an inelastic process with characteristic energies corresponding to the Zeeman splitting. For the σ^+ polarization the electron exchange will be elastic, as the electron orientations in the exciton and in the 2DEG coincide. This effect has been also established in CdTe QW's.[22]

We attribute the reduction of spin-independent exciton broadening in magnetic fields above 4 T (see open triangles in Fig. 10) to a suppression of exciton-electron scattering when the electron spectrum is transformed into discrete Landau levels.[25] From comparison of $\Gamma^X(B=0)$ values in Fig. 8(b) with $\Gamma^{X+}(B=7\ \mathrm{T})$ values in Fig. 9(b) we conclude that for electron densities below $6\times10^{10}\ \mathrm{cm}^{-2}$ exciton-electron scattering is suppressed when the 2DEG is polarized and the exciton has the proper spin orientation (i.e., when the spin of the electron belonging to this exciton is parallel to the 2DEG orientation). The exciton linewidth in this case is dominated by inhomogeneous broadening.

In conclusion, reflectivity spectra were analyzed in detail for *n*-type modulation-doped ZnSe/(Zn,Mg)(S,Se) quantum-well structures. Exciton and trion parameters were determined as a function of the 2DEG density, temperature, and magnetic field, and a relation between exciton and trion oscillator strength was established. A linear dependence of the trion radiative damping on the 2D electron concentration was found. An all-optical method is proposed, which allows us to obtain information about 2DEG's of low density ($<10^{11}\ \mathrm{cm}^{-2}$), namely, to detect its polarization and to determine its density. We found that the effect of an exciton oscillator strength transfer with an increase of the electron density does not exceed 25% of the exciton oscillator strength in undoped QW's. The exciton nonradiative damping has been found to increase rapidly with the 2DEG density, and this increase leads to an exciton line bleaching in reflection spectra. This increase can be attributed to the mechanism of exciton-electron exchange scattering, which in turn is strongly dependent on the carrier spin orientation. ZnSe-based QW's studied show large radiative damping and relatively small nonradiative damping, which allows us to extract parameters of excitonic and trionic resonances with high accuracy. Qualitatively similar behavior of exciton and trion resonances has been observed for CdTe/(Cd,Mg)Te QW's. These results will be presented elsewhere.

ACKNOWLEDGMENTS

The authors are thankful to E. L. Ivchenko for helpful discussions. This work was supported by the NATO Grant No. HTECH.LG 974702, the Deutsche Forschungsgemeinschaft through SFB 410, as well as by the Russian Foundation for Basic Research (Grant No. 98-02-18219).

[1] M. A. Lampert, Phys. Rev. Lett. **1**, 450 (1958).
[2] K. Kheng, R. T. Cox, Y. Merle d'Aubigne, F. Bassani, K. Saminadayar, and S. Tatarenko, Phys. Rev. Lett. **71**, 1752 (1993).
[3] R. T. Cox, V. Huard, K. Kheng, S. Lovisa, R. B. Miller, K. Saminadayar, A. Arnoult, J. Cibert, S. Tatarenko, and M. Potemski, Acta Phys. Pol. A **94**, 99 (1998).
[4] G. Finkelstein, H. Shtrikman, and I. Bar-Joseph, Phys. Rev. Lett. **74**, 976 (1995).
[5] W. Ossau, D. R. Yakovlev, U. Zehnder, G. V. Astakhov, A. V. Platonov, V. P. Kochereshko, J. Nürnberger, W. Faschinger, M. Keim, A. Waag, G. Landwehr, P. C. M. Christianen, J. C. Maan, N. A. Gippius, and S. G. Tikhodeev, Physica B **256-258**, 323 (1998).
[6] G. V. Astakhov, D. R. Yakovlev, V. P. Kochereshko, W. Ossau, J. Nürnberger, W. Faschinger, and G. Landwehr, Phys. Rev. B **60**, R8485 (1999).
[7] S. Glasberg, G. Finkelstein, H. Shtrikman, and I. Bar-Joseph, Phys. Rev. B **59**, R10 425 (1999).
[8] P. Gilliot, D. Brinkmann, J. Kudrna, O. Cregut, R. Levy, A. Arnoult, J. Cibert, and S. Tatarenko, Phys. Rev. B **60**, 5797 (1999).
[9] G. Finkelstein, V. Umansky, I. Bar-Joseph, V. Culin, S. Haacke, J.-D. Ganiere, and B. Deveaud, Phys. Rev. B **58**, 12 637 (1998).
[10] B. Stebe, E. Feddi, A. Ainane, and F. Dujardin, Phys. Rev. B **58**, 9926 (1998), and references therein.
[11] S. Lovisa, R. T. Cox, and K. Saminadayar, Phys. Status Solidi A **164**, 175 (1997).
[12] D. Gekhtman, E. Cohen, Arza Ron, and L. N. Pfeiffer, Phys. Rev. B **54**, 10 320 (1996).

[13] T. Bruhnes, R. Andre, A. Arnoult, J. Cibert, and A. Wasiela, Phys. Rev. B **60**, 11 568 (1999).

[14] P. Kossacki, Acta Phys. Pol. A **94**, 147 (1998).

[15] P. Kossacki, J. Cibert, D. Ferrand, Y. Merle d'Aubigne, A. Arnoult, A. Wasiela, S. Tatarenko, and J. Gaj, Phys. Rev. B **60**, 16 018 (1999).

[16] E. L. Ivchenko, V. P. Kochereshko, P. S. Kopev, V. A. Kosobukin, I. N. Uraltsev, and D. R. Yakovlev, Solid State Commun. **70**, 529 (1989).

[17] E. L. Ivchenko, A. V. Kavokin, V. P. Kochereshko, G. R. Pozina, I. N. Uraltsev, D. R. Yakovlev, R. N. Bicknell-Tassius, A. Waag, and G. Landwehr, Phys. Rev. B **46**, 7713 (1992).

[18] E. L. Ivchenko and G. E. Pikus, in *Superlattices and Other Heterostructures* (Springer, Berlin, 1997), pp. 170, 183.

[19] E. L. Ivchenko and M. Willander, Phys. Status Solidi B **215**, 199 (1999).

[20] E. I. Rashba, Fiz. Tekh. Poluprovodn. [Sov. Phys. Semicond. **8**, 807 (1975)].

[21] J. Feldmann, G. Peter, E. O. Göbel, P. Dawson, K. Moore, C. Foxon, and R. J. Elliott, Phys. Rev. Lett. **59**, 2337 (1987).

[22] V. P. Kochereshko, D. R. Yakovlev, A. V. Platonov, W. Ossau, A. Waag, G. Landwehr, and R. Cox, in *Proceedings of the 23rd International Conference on the Physics of Semiconductors, Berlin, 1996*, edited by M. Scheffler and R. Zimmermann (World Scientific, Singapore, 1996), p. 2135; V. P. Kochereshko, A. V. Platonov, F. Bassani, and R. Cox, Superlattices Microstruct. **24**, 269 (1997).

[23] V. P. Kochereshko, R. A. Suris, D. R. Yakovlev, G. V. Astakhov, W. Ossau, and G. Landwehr (unpublished).

[24] R. B. Miller, T. Baron, R. T. Cox, and K. Saminadayar, J. Cryst. Growth **184/184**, 822 (1998).

[25] V. P. Kochereshko, D. R. Yakovlev, R. A. Suris, W. Ossau, G. Landwehr, T. Wojtowicz, M. Kutrowski, G. Karchewski, and J. Kossut, J. Cryst. Growth **184/185**, 826 (1998).